

LEARNING WHAT TO HEAR: BOOSTING SOUND-SOURCE ASSOCIATION FOR ROBUST AUDIOVISUAL INSTANCE SEGMENTATION

Jinbae Seo¹, Hyeongjun Kwon¹, Kwonyoung Kim¹, Jiyoung Lee^{2*}, and Kwanghoon Sohn^{1,3*}

¹Yonsei University ²Ewha Womans University ³Korea Institute of Science and Technology (KIST)

ABSTRACT

Audiovisual instance segmentation (AVIS) requires accurately localizing and tracking sounding objects throughout video sequences. Existing methods suffer from visual bias stemming from two fundamental issues: uniform additive fusion prevents queries from specializing to different sound sources, while visual-only training objectives allow queries to converge to arbitrary salient objects. We propose Audio-Centric Query Generation using cross-attention, enabling each query to selectively attend to distinct sound sources and carry sound-specific priors into visual decoding. Additionally, we introduce Sound-Aware Ordinal Counting (SAOC) loss that explicitly supervises sounding object numbers through ordinal regression with monotonic consistency constraints, preventing visual-only convergence during training. Experiments on AVISeg benchmark demonstrate consistent improvements: +1.64 mAP, +0.6 HOTA, and +2.06 FSLA, validating that query specialization and explicit counting supervision are crucial for accurate audiovisual instance segmentation. Our code and models are available at <https://github.com/jinbae-s/ACVIS>

Index Terms— Audio-visual instance segmentation, Multimodal Learning, Ordinal regression

1. INTRODUCTION

Humans effortlessly perceive complex scenes by integrating what they see with what they hear. In many real-world scenarios, such as identifying a speaking person in a crowded video, or distinguishing between overlapping instruments in a performance, sound provides critical cues that vision alone cannot resolve as shown in Fig. 1. This motivates the task of audiovisual instance segmentation (AVIS), which aims to segment object instances in the visual scene with their associated audio sources. Early audiovisual learning explored multimodal correspondence through self-supervision [2], evolving from coarse localization [3] to attention-based [4] and contrastive methods [5]. However, these methods are limited to producing only heat maps or bounding boxes rather than semantic-level masks. To address this limitation, audiovisual segmentation emerged with pixel-level precision, starting

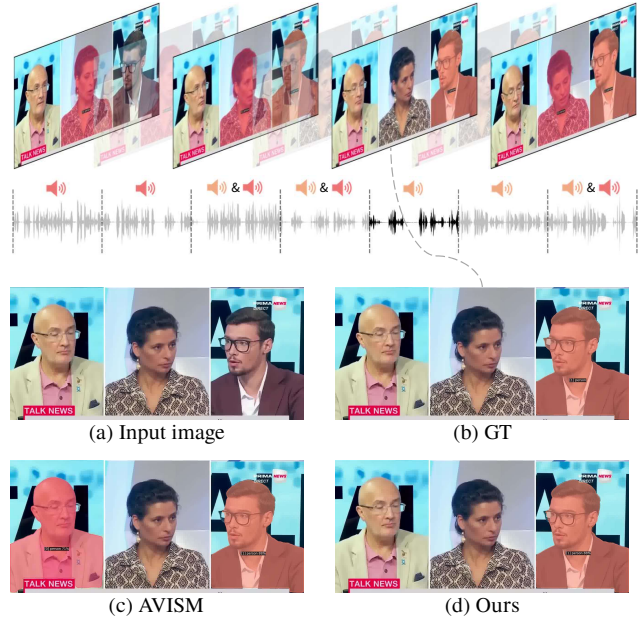


Fig. 1. Visual bias in audiovisual instance segmentation. While ground truth (b) indicates only one person speaking, previous work (AVISM) [1] (c) detects two visible people due to visual dominance. Our ACVIS (d) correctly identifies the speaking person by maintaining audio-visual balance through specialized queries and counting supervision.

with AVS [6, 7] that introduced temporal pixel-wise audio-visual interaction. Subsequent works—AVSegFormer [8] with transformers, SAMA-AVS [9] leverages SAM [10], and VCT [11] with vision-centric queries—improved semantic segmentation but all remained limited to semantic-level, unable to distinguish individual instances. Recently, AVISM [1] has achieved instance-level segmentation through a compacted two-stage architecture: frame-level object localization followed by video-level object tracking. In the first stage, the model predicts frame queries corresponding to instances for each frame by adding audio features to learnable query tokens, which are then refined through visual cross-attention to produce audiovisual frame queries. In the second stage, these frame-level detections are associated across time through a tracker that establishes temporal correspondences between instances. While this approach enables instance-level tracking,

* Corresponding authors.

the frame-level localizer suffers from a critical limitation: audio features are uniformly integrated into all queries through a simple addition process, preventing queries from specializing to different sound sources.

We address the aforementioned limitations through two complementary innovations. First, we replace additive fusion with cross-attention to enable each query to selectively attend to different sound sources in the audio signal. To facilitate better audiovisual correspondence in subsequent decoder layers, our method produces specialized audio-centric queries where each query is pre-assigned to specific audio patterns. Although this modification promotes capturing sound-related instance queries, matching sound sources to instances in complex real-world scenarios, where multiple instances with the same semantic label are loud simultaneously, is highly challenging. Therefore, we introduce a sound-aware ordinal counting (SAOC) loss that provides the missing audio-centric constraint. Explicitly supervising how many queries should activate for sounding objects ensures the decoder optimization considers both visual appearance and audio presence, preventing convergence to visual-only solutions. Our contributions are summarized as:

- We introduce a novel **Audio-Centric audioVisual Instance Segmentation (ACVIS)** for sound source-aware audiovisual instance segmentation, introducing an audio-centric query generator with sound-aware ordinal counting loss.
- Our ACVIS highlights the robustness of query discrimination according to the sound source by ordinal regression through guidance of counting audible objects.
- We demonstrate through experiments where improvements of +1.64 mAP, +0.6 HOTA, and +2.06 FSLA, validating our frame-level innovations as crucial for accurate audio-visual instance segmentation.

2. METHOD

2.1. Problem Formulation and Overview

Audiovisual instance segmentation (AVIS) aims to classify, segment, and track all sounding objects in a given video. Given an input video with audio, the model predicts a set of instance masks with associated class labels.

Our method takes AVISM [1] as a baseline model, which follows the set-prediction paradigm [12, 13] with a two-stage architecture: frame-level object localizer and video-level object tracker. Formally, audio and video encoders extract audio feature f_t^A and visual feature f_t^V for a given input, respectively. The pixel decoder within the object localizer generates enhanced multi-scale features: \bar{f}_t^V for final-resolution map and $\bar{\mathcal{F}}_t^V$ for multi-scale representations. These features, combined with audio features f_t^A and learnable queries \mathbf{q} , produce audiovisual frame queries \mathbf{q}_t^{AV} at frame t . The object tracker aggregates these frame queries $\{\mathbf{q}_t^{AV}\}_{t=1}^T$ into N_v

video queries to generate final predictions $\hat{\mathcal{Y}}$:

$$\mathbf{q}_t^{AV} = \text{ObjLocalizer}(f_t^V, f_t^A, \mathbf{q}) \quad (1)$$

$$\hat{\mathcal{Y}} = \text{ObjTracker}(\{\bar{f}_t^V\}_{t=1}^T, \{f_t^A\}_{t=1}^T, \{\mathbf{q}_t^{AV}\}_{t=1}^T). \quad (2)$$

However, as exemplified in Fig. 1 (c), the baseline often fails to separate sound sources at the instance level. The uniform additive fusion,

$$\mathbf{q}_t^A = \mathbf{q} + \mathbf{1}_{N_f} \otimes f_t^A, \quad \text{where } \mathbf{q} \in \mathbb{R}^{N_f \times D}, f_t^A \in \mathbb{R}^D \quad (3)$$

forces all queries to share identical audio representation, preventing discrimination between instances (e.g., multiple speakers). Furthermore, we speculate that visually concentrated constraints (*i.e.*, mask and classification losses) do not guarantee query specialization to different sound sources. We tackle these problems by introducing (i) an audio-centric query generator (ACQG) that conditions learnable queries directly on audio representations and (ii) a sound-aware ordinal counting (SAOC) loss that explicitly guides the model to detect sounding objects rather than arbitrary visual objects.

2.2. Audio-Centric Frame Queries

To obtain fine-grained audiovisual correspondence at the frame-level, our ACVIS takes each frame and corresponding audio segment as inputs. We also set N_f learnable frame queries $\mathbf{q}_t \in \mathbb{R}^{N_f \times D}$, which derive instance-wise mask in the segmentation decoder. At each time step t , our audio-centric query generator (ACQG) fuses \mathbf{q}_t with the audio feature $f_t^A \in \mathbb{R}^D$ to obtain audio-centric frame queries. ACQG consists of three cross-attention layers:

$$\mathbf{q}_t^A = \text{ACQG}(\mathbf{q}_t, f_t^A, f_t^A) \in \mathbb{R}^{N_f \times D}, \quad (4)$$

where \mathbf{q}_t serves as query and f_t^A as both key and value. This module enables each query to selectively attend to different patterns in the audio signal. Each query thereby selectively attends to different sound sources, creating audio-specialized queries that carry sound-specific priors into the audiovisual frame query generation process.

The segmentation decoder [1] then processes audio-centric frame queries with multi-scale visual features:

$$\mathbf{q}_t^{AV} = \text{Decoder}(\mathbf{q}_t^A, \mathcal{F}_t^V, \mathcal{F}_t^V) \in \mathbb{R}^{N_f \times D}. \quad (5)$$

After processing all frames, the object tracker produces temporally aligned audiovisual frame queries.

2.3. Sound-Aware Ordinal Counting loss

To enhance the sound-source awareness in our framework, we design a count token $q_{\text{cnt}} \in \mathbb{R}^D$ to optimize the weights with our SAOC loss. The count token is concatenated with frame queries, and aggregates the information about the number of sound sources in the object localizer. Following previous work [14], we model counting sound instances as an

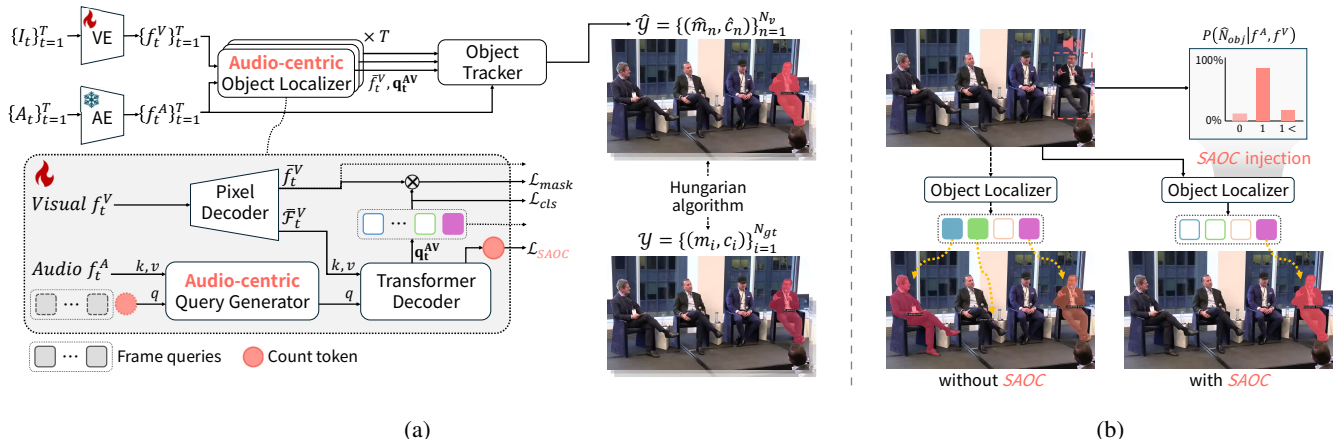


Fig. 2. (a) Overall architecture with audio-centric object localizer and object tracker. Frame queries and count token are processed through our query generator and decoder for AVIS. (b) Our SAOC loss prevents visual bias: without our loss (left), the model over-detects visually salient objects; with our loss (right), only sounding objects are segmented.

ordinal regression problem using conditional probabilities to ensure rank consistency. The count token q_{cnt}^{AV} is processed by $\phi_{cnt} : \mathbb{R}^D \rightarrow \mathbb{R}^{K_{max}}$ to predict:

$$\{p_k\}_{k=0}^{K_{max}-1} = \sigma(\phi_{cnt}(q_{cnt}^{AV})), \quad (6)$$

where $p_0 = P(\hat{N}_{obj} > 0)$ is the marginal probability and $p_k = P(\hat{N}_{obj} > k | \hat{N}_{obj} > k - 1)$ for $k \in \{1, \dots, K_{max} - 1\}$ are conditional probabilities.

Given ground-truth count N_{obj} , we define ordinal targets $t_k = \mathbb{1}[N_{obj} > k]$ and compute our SAOC loss:

$$\mathcal{L}_{SAOC} = -\frac{1}{T} \sum_{t=1}^T \sum_{k=0}^{K_{max}-1} [t_k \log p_k + (1 - t_k) \log(1 - p_k)]. \quad (7)$$

This ordinal formulation enforces monotonic consistency through conditional structure, ensuring $P(\hat{N}_{obj} > k) \geq P(\hat{N}_{obj} > k + 1)$ while providing stable gradients. By explicitly supervising sounding object counts, SAOC prevents the decoder from activating queries for arbitrary visual objects.

2.4. Training and Inference

Training. The object tracker aggregates frame queries $\{q_t^{AV}\}_{t=1}^T$ and uses N_v video queries to generate final mask predictions \hat{Y} . During training, these N_v predictions are matched with ground-truth instance-wise masks via Hungarian algorithm [15]. Frame-level auxiliary heads provide direct supervision on the object localizer outputs. Our ACVIS is optimized with four loss terms, including frame-level masking, video-level masking, frame-video query alignment, and our proposed SAOC losses. Following AVISM [1], \mathcal{L}_{frame} and \mathcal{L}_{video} supervise frame and video-level predictions via bipartite matching respectively, while \mathcal{L}_{sim} aligns query embeddings between frame and video-level across temporal

scales. These visual-centric losses alone often cause over-segmentation of salient objects. To solve this problem, our proposed counting loss \mathcal{L}_{SAOC} optimizes the network to learn audio-aware visual features with audio-centric supervision. To sum up, the overall training objective is:

$$\mathcal{L} = \mathcal{L}_{AVIS} + \lambda_{SAOC} \mathcal{L}_{SAOC}, \quad (8)$$

where λ_{SAOC} is the hyperparameter for \mathcal{L}_{SAOC} and \mathcal{L}_{AVIS} is the weighted sum of \mathcal{L}_{frame} , \mathcal{L}_{video} and \mathcal{L}_{sim} .

Inference. During inference, the N_v video-level predictions are filtered through confidence thresholding to produce N_{pred} final instance trajectories $\hat{Y} = \{(\hat{m}_n, \hat{c}_n)\}_{n=1}^{N_{pred}}$, where each instance spans multiple frames with mask $\hat{m}_n \in [0, 1]^{T \times H \times W}$ and class logits $\hat{c}_n \in \mathbb{R}^{K+1}$.

3. EXPERIMENTS

3.1. Experimental Settings

Datasets. We evaluate on AVISeg benchmark containing 926 videos (16 hours, 61.4s average), 94,074 instance masks across 56,871 frames in 26 categories. Each video is divided into 1 fps clips, and only objects that emit sound are exhaustively annotated with persistent identifiers while silent instances are not masked.

Metrics. Following [1], we report three primary metrics that jointly assess detection, localization, and identity association over time. While mAP [16] is computed on video trajectories using spatio-temporal IoU, HOTA [17] jointly measures detection and association through frame-wise bijective matching and sequence-level scoring. FSLA [1] is the fraction of correct frames after bipartite matching, requiring matched counts/categories and per-object IoU $\geq \alpha$, averaged over $\alpha \in \{0.05, 0.10, \dots, 0.95\}$. We also report FSLA for silent, single-source, and multi-source frames (FSLAn/s/m).

Implementation details. Following AVISM protocol, we use ResNet-50 [18] for visual and VGGish [19] for audio. We

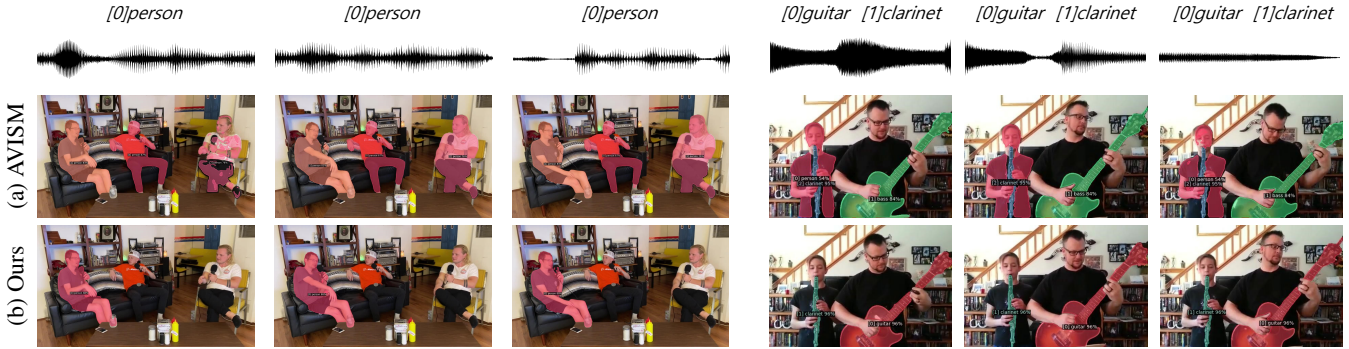


Fig. 3. Qualitative results across diverse audio scenarios with varying sound sources.

Model	mAP	HOTA	FSLA	FSLAn	FSLAs	FSLAm
AVISM	45.04	64.52	44.42	20.62	32.62	54.99
ACVIS	46.68	65.12	46.48	10.74	34.45	58.81

Table 1. Performance comparisons with SoTAs.

ACQG	\mathcal{L}_{SAOC}	mAP	HOTA	FSLA
✓		45.17	63.27	45.45
✓	✓	46.68	65.12	46.48

Table 3. Impact of audio-centric query generator and \mathcal{L}_{SAOC}

resize the shorter image side to 360 pixels during training and 448 pixels at inference, keeping aspect ratio. Our model uses $N_f = 100$ frame queries and $N_v = 100$ video queries with a window size $W = 6$ in the video-level tracker. We set all loss weights to 1.0, except the weight of \mathcal{L}_{sim} , which is 0.5.

3.2. Main Results

As shown in Table 1, our ACVIS improves overall detection and tracking quality over the baseline, raising mAP from 45.04 to 46.68 (+1.64), HOTA from 64.52 to 65.12 (+0.60), and FSLA from 44.42 to 46.48 (+2.06). On the decomposed FSLA scores, our method favors sounding-object localization in both single-source and multi-source frames, with gains on FSLAs (+1.83) and FSLAm (+3.82). Figure 3 shows reduced mask coalescence and identity swaps in crowded scenes.

3.3. Ablation Studies

Audio-centric query generator and \mathcal{L}_{SAOC} . Table 3 shows that adding \mathcal{L}_{SAOC} to ACQG improves all metrics: mAP 45.17 to 46.68 (+1.51), HOTA 63.27 to 65.12 (+1.85), and FSLA 45.45 to 46.48 (+1.03). This indicates that audio-conditioned queries and ordinal counting provide complementary benefits.

Loss design. Replacing standard cross-entropy with \mathcal{L}_{SAOC} consistently improves performance (Table 4): mAP 44.45 to 46.68 (+2.23), HOTA 63.95 to 65.12 (+1.17), and FSLA 44.00 to 46.48 (+2.48). The ordinal formulation better

Backbone	Pre-trained dataset	mAP	HOTA	FSLA
ResNet-50	IN	42.14	62.09	42.87
ResNet-50	IN+COCO	46.68	65.12	46.48
Swin-L	IN+COCO	54.16	72.96	54.17

Table 2. Impact of visual backbone and pre-training dataset.

Loss type	mAP	HOTA	FSLA
\mathcal{L}_{CE}	44.45	63.95	44.00
\mathcal{L}_{SAOC}	46.68	65.12	46.48

Table 4. Impact of the choice of loss.

K_{max}	mAP	HOTA	FSLA
2	46.68	65.12	46.48
3	45.23	64.67	44.90
4	44.94	64.01	44.06

Table 5. Impact of K_{max}

ranks hypotheses, stabilizing matching and reducing identity switches.

Backbone and pretraining dataset. Pretraining on ImageNet [20] and COCO [21], rather than ImageNet alone, yields clear improvements (Table 2): mAP 42.14 to 46.68 (+4.54), HOTA 62.09 to 65.12 (+3.03), and FSLA 42.87 to 46.48 (+3.61). Replacing ResNet-50 with Swin-L [22] is expected to further improve segmentation quality and long-range identity maintenance.

Sensitivity to K_{max} . Table 5 analyzes different K_{max} values for SAOC loss. Setting $K_{max} = 2$ performs best, aligning with the dataset’s typical sounding object distribution, while higher values reduce accuracy.

4. CONCLUSION

We presented audio-centric query generation and sound-aware ordinal counting loss to address visual dominant regime in audiovisual instance segmentation. Our method enables queries to specialize to different sound sources, while SAOC loss explicitly supervises sounding object counts via ordinal regression. Comprehensive experiments demonstrate that both query specialization and counting supervision are essential, achieving strongest gains in challenging multi-source scenario. These results validate that balanced frame-level processing via both architectural and objective design is crucial for accurate audiovisual instance segmentation.

5. REFERENCES

- [1] Ruohao Guo, Xianghua Ying, Yaru Chen, Dantong Niu, Guangyao Li, Liao Qu, Yanyu Qi, Jinxing Zhou, Bowei Xing, Wenzhen Yue, et al., “Audio-visual instance segmentation,” in *Proceedings of the Computer Vision and Pattern Recognition Conference*, 2025, pp. 13550–13560.
- [2] Relja Arandjelovic and Andrew Zisserman, “Look, listen and learn,” in *Proceedings of the IEEE international conference on computer vision*, 2017, pp. 609–617.
- [3] Arda Senocak, Tae-Hyun Oh, Junsik Kim, Ming-Hsuan Yang, and In So Kweon, “Learning to localize sound source in visual scenes,” in *Proceedings of the IEEE conference on computer vision and pattern recognition*, 2018, pp. 4358–4366.
- [4] Rui Qian, Di Hu, Heinrich Dinkel, Mengyue Wu, Ning Xu, and Weiyao Lin, “Multiple sound sources localization from coarse to fine,” in *European Conference on Computer Vision*. Springer, 2020, pp. 292–308.
- [5] Honglie Chen, Weidi Xie, Triantafyllos Afouras, Arsha Nagrani, Andrea Vedaldi, and Andrew Zisserman, “Localizing visual sounds the hard way,” in *Proceedings of the IEEE/CVF conference on computer vision and pattern recognition*, 2021, pp. 16867–16876.
- [6] Jinxing Zhou, Jianyuan Wang, Jiayi Zhang, Weixuan Sun, Jing Zhang, Stan Birchfield, Dan Guo, Lingpeng Kong, Meng Wang, and Yiran Zhong, “Audio-visual segmentation,” in *European Conference on Computer Vision*. Springer, 2022, pp. 386–403.
- [7] Jinxing Zhou, Xuyang Shen, Jianyuan Wang, Jiayi Zhang, Weixuan Sun, Jing Zhang, Stan Birchfield, Dan Guo, Lingpeng Kong, Meng Wang, et al., “Audio-visual segmentation with semantics,” *International Journal of Computer Vision*, vol. 133, no. 4, pp. 1644–1664, 2024.
- [8] Shengyi Gao, Zhe Chen, Guo Chen, Wenhai Wang, and Tong Lu, “Avsegformer: Audio-visual segmentation with transformer,” in *Proceedings of the AAAI conference on artificial intelligence*, 2024, vol. 38, pp. 12155–12163.
- [9] Jinxiang Liu, Yu Wang, Chen Ju, Chaofan Ma, Ya Zhang, and Weidi Xie, “Annotation-free audio-visual segmentation,” in *Proceedings of the IEEE/CVF Winter Conference on Applications of Computer Vision*, 2024, pp. 5604–5614.
- [10] Alexander Kirillov, Eric Mintun, Nikhila Ravi, Hanzi Mao, Chloe Rolland, Laura Gustafson, Tete Xiao, Spencer Whitehead, Alexander C Berg, Wan-Yen Lo, et al., “Segment anything,” in *Proceedings of the IEEE/CVF international conference on computer vision*, 2023, pp. 4015–4026.
- [11] Shaofei Huang, Rui Ling, Tianrui Hui, Hongyu Li, Xu Zhou, Shifeng Zhang, Si Liu, Richang Hong, and Meng Wang, “Revisiting audio-visual segmentation with vision-centric transformer,” in *Proceedings of the Computer Vision and Pattern Recognition Conference*, 2025, pp. 8352–8361.
- [12] Nicolas Carion, Francisco Massa, Gabriel Synnaeve, Nicolas Usunier, Alexander Kirillov, and Sergey Zagoruyko, “End-to-end object detection with transformers,” in *European conference on computer vision*. Springer, 2020, pp. 213–229.
- [13] Bowen Cheng, Ishan Misra, Alexander G Schwing, Alexander Kirillov, and Rohit Girdhar, “Masked-attention mask transformer for universal image segmentation,” in *Proceedings of the IEEE/CVF conference on computer vision and pattern recognition*, 2022, pp. 1290–1299.
- [14] Xintong Shi, Wenzhi Cao, and Sebastian Raschka, “Deep neural networks for rank-consistent ordinal regression based on conditional probabilities,” *Pattern Analysis and Applications*, vol. 26, no. 3, pp. 941–955, 2023.
- [15] Harold W Kuhn, “The hungarian method for the assignment problem,” *Naval research logistics quarterly*, vol. 2, no. 1-2, pp. 83–97, 1955.
- [16] Linjie Yang, Yuchen Fan, and Ning Xu, “Video instance segmentation,” in *Proceedings of the IEEE/CVF international conference on computer vision*, 2019, pp. 5188–5197.
- [17] Jonathon Luiten, Aljosa Osep, Patrick Dendorfer, Philip Torr, Andreas Geiger, Laura Leal-Taixé, and Bastian Leibe, “Hota: A higher order metric for evaluating multi-object tracking,” *International journal of computer vision*, vol. 129, no. 2, pp. 548–578, 2021.
- [18] Kaiming He, Xiangyu Zhang, Shaoqing Ren, and Jian Sun, “Deep residual learning for image recognition,” in *Proceedings of the IEEE conference on computer vision and pattern recognition*, 2016, pp. 770–778.
- [19] Shawn Hershey, Sourish Chaudhuri, Daniel PW Ellis, Jort F Gemmeke, Aren Jansen, R Channing Moore, Manoj Plakal, Devin Platt, Rif A Saurous, Bryan Seybold, et al., “Cnn architectures for large-scale audio classification,” in *2017 IEEE international conference on acoustics, speech and signal processing (icassp)*. IEEE, 2017, pp. 131–135.

- [20] Jia Deng, Wei Dong, Richard Socher, Li-Jia Li, Kai Li, and Li Fei-Fei, “Imagenet: A large-scale hierarchical image database,” in *2009 IEEE conference on computer vision and pattern recognition*. Ieee, 2009, pp. 248–255.
- [21] Tsung-Yi Lin, Michael Maire, Serge Belongie, James Hays, Pietro Perona, Deva Ramanan, Piotr Dollár, and C Lawrence Zitnick, “Microsoft coco: Common objects in context,” in *European conference on computer vision*. Springer, 2014, pp. 740–755.
- [22] Ze Liu, Yutong Lin, Yue Cao, Han Hu, Yixuan Wei, Zheng Zhang, Stephen Lin, and Baining Guo, “Swin transformer: Hierarchical vision transformer using shifted windows,” in *Proceedings of the IEEE/CVF international conference on computer vision*, 2021, pp. 10012–10022.